Extreme Mechanics Letters 12 (2017) 30–36

Contents lists available at ScienceDirect

Extreme Mechanics Letters

journal homepage: www.elsevier.com/locate/eml

Coupling local resonance with Bragg band gaps in single-phase mechanical metamaterials

A.O. Krushynska [a,*], M. Miniaci [b], F. Bosia [a], N.M. Pugno [c,d,e]

[a] Department of Physics and Nanostructured Interfaces and Surfaces Inter-departmental Centre, University of Turin, 10125, Turin, Italy

[b] University of Le Havre, Laboratoire Ondes et Milieux Complexes, UMR CNRS 6294, 76600 Le Havre, France

[c] Laboratory of Bio-Inspired and Graphene Nanomechanics, Department of Civil, Environmental and Mechanical Engineering, University of Trento, 38123, Trento, Italy

[d] Center for Materials & Microsystems, Fondazione Bruno Kessler, 38123, Trento, Italy

[e] School of Engineering and Materials Science, Queen Mary University of London, E1 4NS, London, United Kingdom

ARTICLE INFO

Article history:
Received 29 February 2016
Received in revised form
4 August 2016
Accepted 8 October 2016
Available online 21 October 2016

Keywords:
Mechanics
Wave propagation
Mechanical metamaterials
Bragg scattering
Local resonance
Wave dispersion
Time transient analysis
Finite element method

ABSTRACT

Various strategies have been proposed in recent years in the field of mechanical metamaterials to widen band gaps emerging due to either Bragg scattering or to local resonance effects. One of these is to exploit coupled Bragg and local resonance band gaps. This effect has been theoretically studied and experimentally demonstrated in the past for two- and three-phase mechanical metamaterials, which are usually complicated in structure and suffer from the drawback of difficult practical implementation. To avoid this problem, we theoretically analyze for the first time a single-phase solid metamaterial with so-called quasi-resonant Bragg band gaps. We show evidence that the latter are achieved by obtaining an overlap of the Bragg band gap with local resonance modes of the *matrix* material, instead of the inclusion. This strategy appears to provide wide and stable band gaps with almost unchanged width and frequencies for varying inclusion dimensions. The conditions of existence of these band gaps are characterized in detail using metamaterial models. Wave attenuation mechanisms are also studied and transmission analysis confirms efficient wave filtering performance. Mechanical metamaterials with quasi-resonant Bragg band gaps may thus be used to guide the design of practically oriented metamaterials for a wide range of applications.

1. Introduction

Mechanical metamaterials are engineered periodic composites with exceptional dynamic properties. The possibility they provide to manipulate and attenuate elastic waves at various frequencies can be exploited for various applications, ranging from seismic shielding [1,2] or noise abatement [3] to subwavelength imaging [4] and thermal management [5]. These fundamental properties arise from metamaterial geometry and/or composition and are due to the existence of band gaps (BGs)—frequency ranges, in which wave propagation is inhibited. The frequencies and width of BGs depend on the contrast between mechanical properties of material phases and lattice parameters. Bragg BGs occur in Phononic Crystals (PCs) through destructive interference of waves scattered from periodic inhomogeneities at wavelengths comparable to the spatial periodicity of the lattice [6,7]. The resulting high operating frequencies make this type of structure unsuitable for noise mitigation or vibration isolation. Instead, hybridization BGs [8,9] are typically induced in metamaterials by resonant modes of the constituents, which interact with the wave field in the embedding medium [10]. These BGs are independent of the spatial configuration of the metamaterial and can be nucleated at much lower frequencies than Bragg BGs, but are usually rather narrow and require heavy resonators [10–14]. Thus, due to their complicated design or limited working performance [13,15,16], mechanical metamaterials are yet to become widespread in applications.

One promising solution to overcome these limitations is to exploit overlapping Bragg and local resonance BGs. The co-existence of both BG types in the same structure has already been demonstrated theoretically and experimentally for different systems at various frequencies [17–23], including in 3D sonic solid metamaterials with coated inclusions [24,25]. These studies

* Correspondence to: Department of Physics, University of Turin, Via P. Giuria 1, 10125, Turin, Italy.
E-mail address: akrushynska@gmail.com (A.O. Krushynska).

http://dx.doi.org/10.1016/j.eml.2016.10.004
2352-4316/

highlight the BG formation mechanisms [9,17,22,23] and show that the coupling between the two BGs leads to the creation of a combined 'resonant Bragg' BG with a broad transmission gap in the sub-wavelength region [7,21,22,24,25]. These conclusions are also valid for surface guided waves [26] and acoustic waves in PCs with gas bubbles [27]. Recently, coupled resonant Bragg BGs have also been found in co-continuous metamaterials with enhanced mechanical properties [28]. All these studies involve composite metamaterial structures comprising at least two material phases, and the hybridization BG is usually associated with resonance modes of inclusions.

A more practical and promising solution are single-phase metamaterials, which have attracted increasing interest in the community [29–38], and in which both types of BGs have been shown to be present [39–43]. However, to the best of our knowledge, the conditions and physical mechanism of the coupling of Bragg BG with local resonances in single-phase structures has not yet been analyzed. In this work, we present evidence for single-phase 2-D and 3-D slab-type metamaterials with wide BGs due to the interaction between Bragg scattering and resonant modes. Moreover, we develop a new strategy to bring the BGs to overlap, using resonating modes of the matrix material instead of the inclusions, leading to so-called 'quasi-resonant Bragg' BGs. These BGs appear to exhibit efficient wave attenuation and stable frequency ranges for a wide range of geometric parameters of the inclusions. Thus, the proposed strategy shows promise for enhanced wave attenuation mechanisms coupled with the possibility of fabricating simpler structures, promoting the exploitation of mechanical metamaterials in real applications.

2. Two-dimensional mechanical metamaterials

2.1. Two-phase structures

First, we analyze 2-D phononic structures, in which pure transverse (out-of-plane) and mixed (in-plane) modes propagate independently, when the wave vector $\vec{k}$ is restricted to the XY plane. In this Section, we analyze in-plane modes only.

We start by considering a square array of circular steel inclusions (Fig. 1(a)) or cavities (Fig. 1(b)) in a typical polymeric material, such as that used in a 3-D printer, characterized by Young's modulus $E = 2$ GPa, Poisson's ratio $\nu = 0.4$ and mass density $\rho = 1050$ kg/m^3. The material parameters of isotropic steel are Young's modulus $E = 207$ GPa, Poisson's ratio $\nu = 0.3$, and mass density $\rho = 7784$ kg/m^3. As a first approximation, we neglect any dissipation losses. We consider the cavities to be filled by vacuum, so that no refraction of elastic waves occurs at their boundary. The radius of an inclusion or a cavity is R, and the distance between the centers of two neighboring non-diagonal inclusions or cavities is a. Fig. 1 shows the corresponding band structures for wave numbers varying along the boundary of the first Brillouin zone Γ–X–M evaluated by the Finite Element Method (FEM) for a representative unit cell with $a = 1$ mm and $R = 0.45\,a$. Blue and red curves indicate propagating and evanescent modes with real and imaginary values of the wave vector, respectively. The simulations are performed by applying Bloch periodic conditions at the unit cell boundaries and implemented using the commercial software COMSOL Multiphysics 4.3. The frequencies f are normalized as $\Omega = fa/c_t$, c_t being the transverse wave velocity. Directional and complete BGs are indicated by red and green shaded rectangles, respectively.

For the PC with steel inclusions (Fig. 1(a)), the wide complete band gap occurring between the third, $\Omega = 0.727$, and fourth, $\Omega = 2.071$, pass bands is due to Bragg scattering. Vibration forms at the BG bounds show localization of motion in the matrix material. The BG in the PC with cavities (Fig. 1(b)) is smaller in size and shifted to lower frequencies. The shift can be explained by the lower rigidity of the phononic structure, while the decrease of the BG size occurs due to the presence of localized modes, e.g. the fourth pass band, forming the upper BG bound. Although the vibration forms at the BG bounds shown in subfigures of Fig. 1 differ for the two considered structures, the BG in a PC with cavities is also due to the Bragg scattering mechanism. This can be deduced from the structure of the imaginary part of the spectrum, typical for Bragg BGs, which uniformly varies within the BG with a maximum value approximately at its mid-frequency [44], and from the similarity in the pass bands below the BGs.

Next, we analyze a metamaterial composed of polymeric circular cylinders with steel cores, which are connected by means of thin ligaments (schematically shown in the inset of Fig. 2). The radius of the steel inclusion is $R_{inc} = 0.25a$, the radius of the coated inclusion is $r = 0.35a$, and the thickness of the ligaments is $b = 0.05a$, where a is defined as previously. The corresponding band structure shown in Fig. 2 is characterized by three wide BGs separated by almost flat bands due to localized modes (the corresponding vibration patterns are shown in subfigures of Fig. 2). It is difficult to ascertain the physical nature of the BGs with certainty. On one hand, the imaginary part of the lowest BG resembles that expected for Bragg scattering (see e.g. Fig. 1); however, a localized mode occurs at the BG lower bound, when the coated steel cylinder vibrates as a rigid mass with the ligaments playing the role of springs. Below this mode, there is a pass band characterized by torsional motions of the coated cylinders, which are also typical for locally resonant materials [13]. Thus, the BG appears to be due to coupled Bragg and local resonance effects, as its large size also indicates. However, this metamaterial configuration is unpractical due to manufacturing difficulties and stability issues.

To stiffen the whole structure, we combine it with the previously considered PC with cavities. The resulting configuration is schematically shown in Fig. 3 together with the corresponding band diagram. This metamaterial is characterized by three BGs. The lowest BG bound is of the local resonance type and consists in a localized mode $\Omega = 0.182$ with the vibration pattern shown in Fig. 3, similar to that occurring in the BG in the coated cylinders lattice (see Fig. 2). The resonance nature of this BG is confirmed by the structure of the imaginary part of the diagram, typical for locally resonant metamaterials [45]. The third BG around $\Omega = 1.5$ is due to Bragg scattering, as indicated by the Bragg-type imaginary bands.

The second (widest) BG has a lower bound at the same frequencies as the Bragg BG of the PC with cavities, while its upper bound is at about twice that of the PC with cavities. The vibration pattern at the lower bound of the BG appears to be a combination of localized motions in thin ligaments (vibration pattern at $\Omega = 0.732$ in Fig. 2) and vibrations of the rhombus-shaped material portions originating from the PC with cavities. Therefore, at the lower bound of the second BG, the matrix sections oscillate as rigid bodies, while the coated inclusions are motionless. The localized motions in the matrix are similar to those in the inclusions also for torsional vibrations of rhombus-shaped matrix portions corresponding to the mode below the lower BG bound (vibration pattern at $\Omega = 0.532$ in Fig. 3). The described behavior is similar to local resonances at the lower bound of the lowest BG. However, the structure of the imaginary parts of the spectrum is totally different and shows enhanced wave attenuation typical for the coupled 'resonance-Bragg' BGs [7,24].

All the mentioned features suggest a new BG formation mechanism: the local resonances of the rhombus-shaped (matrix) parts are coupled with Bragg scattering in the same parts of the metamaterial. The presence of coated inclusions allows the localizing of the motions in the matrix and shifting the upper bound of the BG to higher frequencies by stiffening the whole structure.

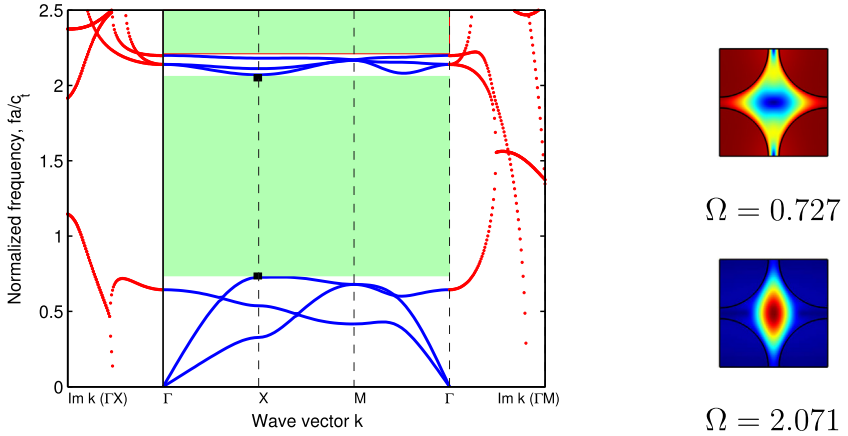

(a) PC with steel inclusions.

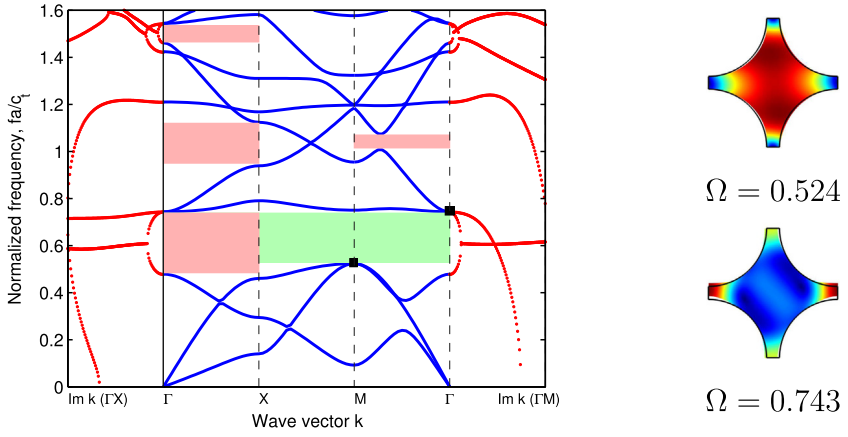

(b) PC with circular cavities.

Fig. 1. Band structures and vibration patterns for 2-D PCs with circular (a) steel inclusions and (b) cavities. The complete and directional band gaps are shaded in green and red, respectively. In vibration patterns, displacements are represented in a color scale from red (maximum) to blue (minimum). (For interpretation of the references to color in this figure legend, the reader is referred to the web version of this article.)

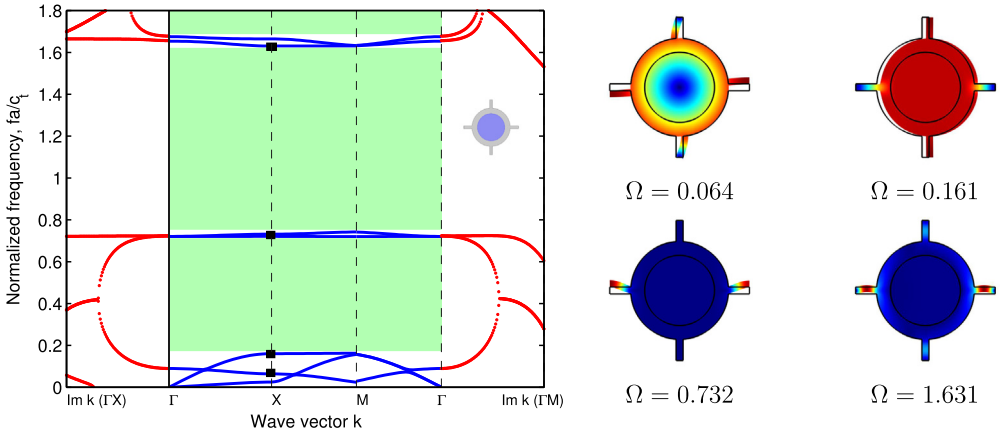

Fig. 2. Band structure and vibration forms for a 2-D phononic structure made of circular cylinders with steel cores connected by thin ligaments.

The fact than local resonances are induced only in the matrix distinguishes the considered metamaterial structure from other phononic structures with coupled 'resonance-Bragg' BGs [7,22,24,28], where Bragg scattering in the matrix is coupled with local resonances in the inclusions. Due to this difference, we denote this type of BG as a 'quasi-resonant Bragg' BG. Notice that there is no separate local resonance BG in the matrix, since resonances emerge only after introducing the inclusions. At the same time, the wide BG in Fig. 3 is located at the same frequencies as the Bragg BG in Fig. 1.

2.2. Single-phase structures

To examine a single-phase configuration, we replace the steel inclusion in the previously considered 2-phase model with the polymeric material. The corresponding computed band structure is shown in Fig. 4. The lowest BG originating from the local resonance effect in the 2-phase configuration (Fig. 3) disappears, since the mass of the inclusion is insufficient to induce this BG. The two higher complete BGs found for the 2-phase metamaterial are preserved and approximately retain their width: e.g., for the single-

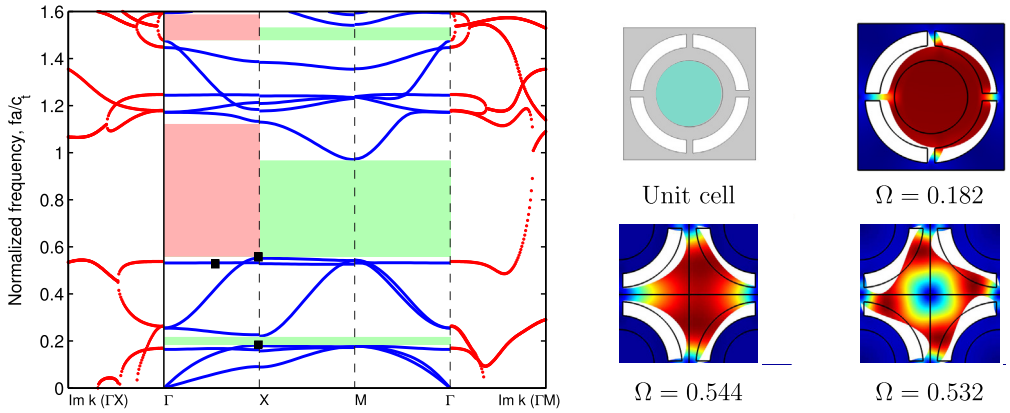

Fig. 3. Band structure, representative unit cell and vibration patterns for a metamaterial with a 2-phase inclusion.

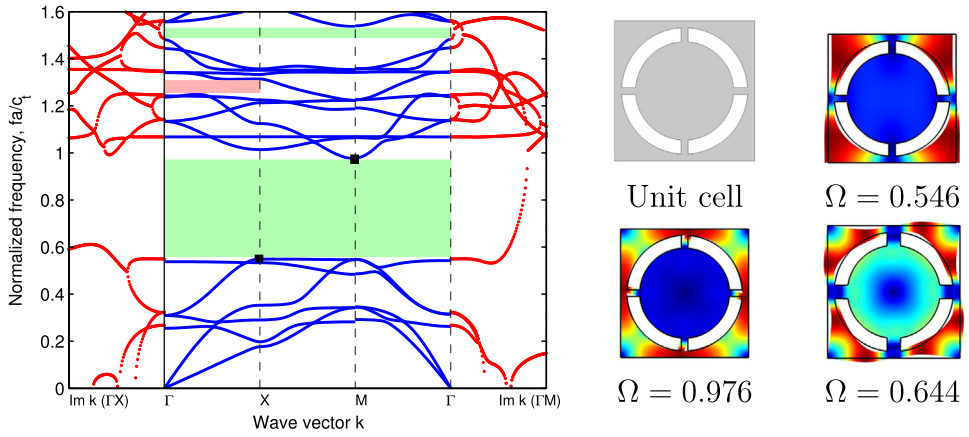

Fig. 4. Band structure, representative unit cell and vibration forms for a 2-D single-phase metamaterial with a quasi-resonant Bragg BG. Vibration form at $\Omega = 0.644$ corresponds to the lower bound of the BG in the same metamaterial with 2 times thicker ligaments compared to the shown unit cell.

phase metamaterial the lowest BG spans from $\Omega = 0.546$ to 0.976 and corresponds to the BG frequencies between 0.553 and 0.975 for the 2-phase metamaterial. The structure of the imaginary part shows that the physical mechanism of these BGs is also preserved: the wide BG is of a 'quasi-resonant Bragg' type with enhanced wave attenuation indicated by large non-uniformly varying values of the imaginary wave part of the spectrum, whereas the higher BG is of Bragg-type. This indicates that overlapping Bragg BG with the local resonances in the matrix can be achieved in single-phase metamaterials.

Comparing 1- and 2-phase models, it appears that the mass of the inclusion does not play a key role in the formation mechanism of the coupled BG. This also follows from the examination of the vibration patterns at the BG bounds, $\Omega = 0.564$ and 0.976 in Fig. 4, in which the circular inclusion is motionless. To determine the influence of the inclusion geometric parameters on the BG frequencies, we calculated band diagrams for an inclusion with thicker, $b = 0.1a$, and thinner, $b = 0.025$, ligaments, as well as for an inclusion of smaller radius, $r = 0.25a$, keeping other dimensions unchanged. The quasi-resonant Bragg BG for the inclusions with smaller radius and thinner ligaments appears at approximately the same frequencies (0.538–0.922 and 0.533–1.068, respectively). For the unit cell with the thicker ligaments, the band gap is at $\Omega = 0.644$–1.038. In the latter case, the decrease in the BG width can be explained by the fact that thicker ligaments make the structure stiffer and involve the inclusions in the matrix vibration, as clearly seen in the vibration form at $\Omega = 0.644$ in Fig. 4(e), corresponding to the lower BG bound (to be compared with the pattern at $\Omega = 0.546$ in Fig. 4 for the structure with 2 times thinner ligaments). The parametric study shows that for the proposed configuration, the optimal ligament thickness to achieve the widest quasi-resonant Bragg BG is $b < 0.1$.

On the other hand, thin ligaments in combination with a small inclusion may result in the decrease of the BG size due to the appearance of resonance modes of the inclusion at previously forbidden frequencies. For example, Fig. 5 shows a band diagram for a single-phase metamaterial with $R = 0.45a$, $r = 0.25a$, and $b = 0.025$. The lower BG bound is again related to a mode with motions concentrated outside the inclusion (vibration pattern at $\Omega = 0.524$ in Fig. 5), while the upper bound is a flat curve representing a mode with vibrations localized in the ligaments only (vibration pattern at $\Omega = 0.904$ in Fig. 5) and differs from that for the previously considered configuration (vibration pattern at $\Omega = 0.976$ in Fig. 4). Other modes above the BG are also almost flat curves characterized by vibrations of the ligaments similar to that at $\Omega = 0.923$ in Fig. 5. Besides the decrease in the BG size, another negative effect of the appearance of modes localized in the ligaments is the vanishing of the coupled resonance-Bragg effect observed due to the changes in the imaginary part of the spectrum. The imaginary curves in Fig. 5 resemble those obtained for Bragg scattering as in Fig. 1, rather than those describing enhanced wave attenuation in Fig. 4. Therefore, to obtain enhanced wave attenuation, coupling between the quasi-resonant Bragg BG with local resonances of the ligaments should be eliminated.

3. 3D slab-type single-phase metamaterials

The procedure developed for obtaining quasi-resonant Bragg BGs for 2-D models is now applied to 3D slab structures. We consider the metamaterials with similar cross-sections as the

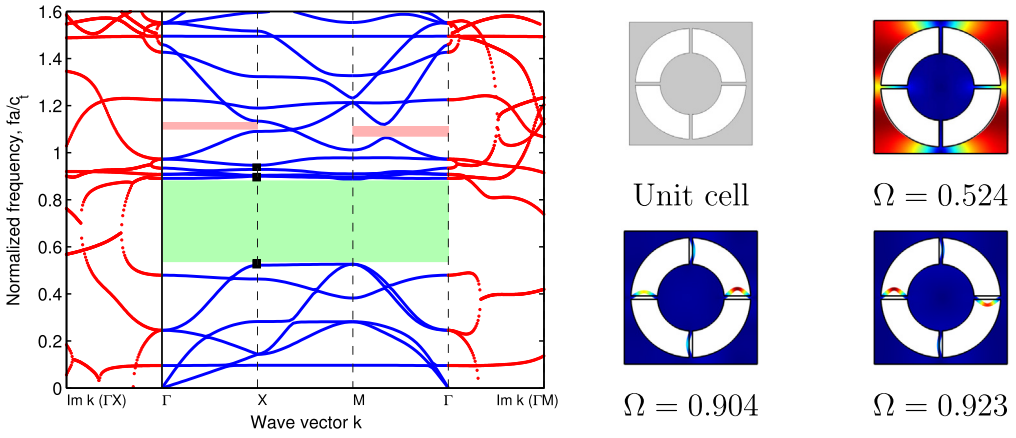

Fig. 5. Band structure, representative unit cell and vibration forms for a 2-D single-phase metamaterial with thinner ligaments and smaller inclusion compared to the case shown in Fig. 4.

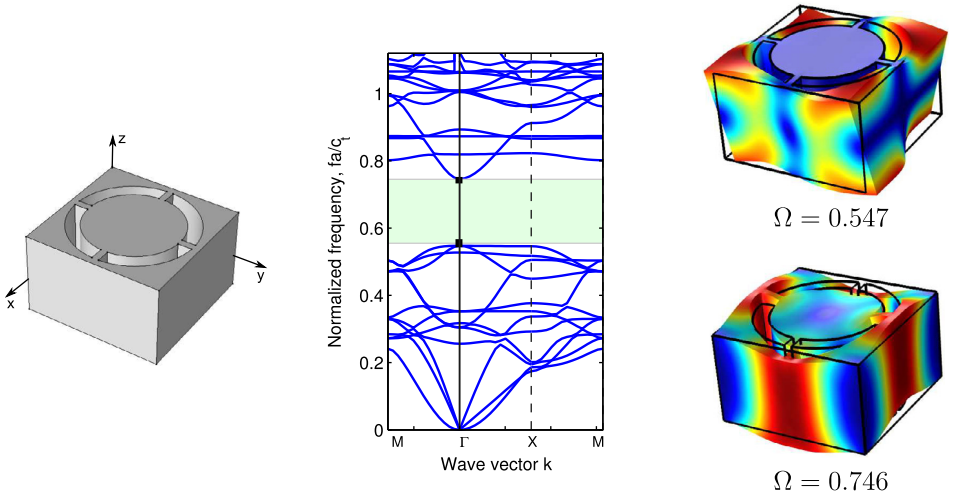

Fig. 6. (left) Representative unit cell and (center) band structure for a plate-type single-phase metamaterial with a quasi-resonant Bragg BG indicated by the shaded region; (right) vibration patterns at the lower and upper bounds of the BG.

previously analyzed 2-D cases, adding the thickness along the z axis to obtain a plate metamaterial configuration. The cross-sectional dimensions are $R = 0.45a$, $r = 0.35a$ and $b = 0.05a$, and the plate thickness is designated as h. The parametric study for various values of h shows that the value $h = 0.6a$ provides the maximum BG size for $0.1a \leq h \leq a$.

The band diagram for the mentioned parameters is shown in Fig. 6(b). The BG is located at slightly lower frequencies compared to the corresponding 2-D case (see Fig. 4), due to the coupling with out-of-plane modes, as deduced from analysis of the vibration patterns at the BG bounds in Fig. 6, both of which indicate strong dependence on the z coordinate. These vibration shapes also point out that the BG is of a 'quasi-resonant Bragg' type, since at the BG bounds the inclusion is almost motionless, while the matrix parts vibrate intensively. Also, as in the 2-D case, the BG is located at the Bragg BG frequencies and is much wider compared to the one found for a plate with cylindrical cavities of the same radius (located between $\Omega = 0.530$ and $\Omega = 0.552$). Moreover, simulations reveal that variations of the in-plane inclusion parameters do not influence the BG significantly. Thus, we may conclude that quasi-resonant Bragg BGs are also found in plate-type single-phase metamaterials.

Finally, in order to confirm the band structure analysis, transmission spectra are calculated for wave propagation in a $400 \times 200 \times 0.6$ mm^3 homogeneous plate with metamaterial regions composed by the unit cells from Fig. 6(a) around an area of 2×2 mm^2, as shown in Fig. 7(a). The cavity has been introduced to replicate a possible experimental test in which a finite surface is required to attach a sensor to measure the displacements. Simulations are performed in ABAQUS with a mesh of over 1 million linear hexahedral C3D8R elements, in order to provide accuracy up to the maximum frequency of interest. An excitation is applied to the surface at point E in Fig. 7(a) by imposing a displacement of 1×10^{-6} mm in the out-of-plane direction z. Two input signals are considered: (i) a sum of Hanning modulated 7 sine cycles centered at 250, 375, 500, 675 and 750 kHz (time evolution and FFT are shown in Fig. 7(b), left) and (ii) a Hanning modulated 21 sine cycles centered at 550 kHz (Fig. 7(b), right). The transient explicit simulations are 1×10^{-4} s long to allow wave reflections from all the plate edges resulting in multiple waves impinging the metamaterial region from different directions.

Fig. 7(c, d) illustrate the transmitted displacements $U1$ and $U3$ along the x and z directions, respectively, recorded at point A for elastic waves propagating in the MetaMaterial Plate (MMP) compared to those in a homogeneous plate (HP) for reference. Transmission spectra obtained by assigning the excitation pulse (i), are presented in both time and frequency domains. Results show a frequency range extending from 480 to 630 kHz in which the attenuation in the MMP is so strong that it can be treated as a complete band gap. These frequencies are slightly higher than those obtained in the dispersion analysis, since the latter are relative to an infinite metamaterial. The filtering abilities of

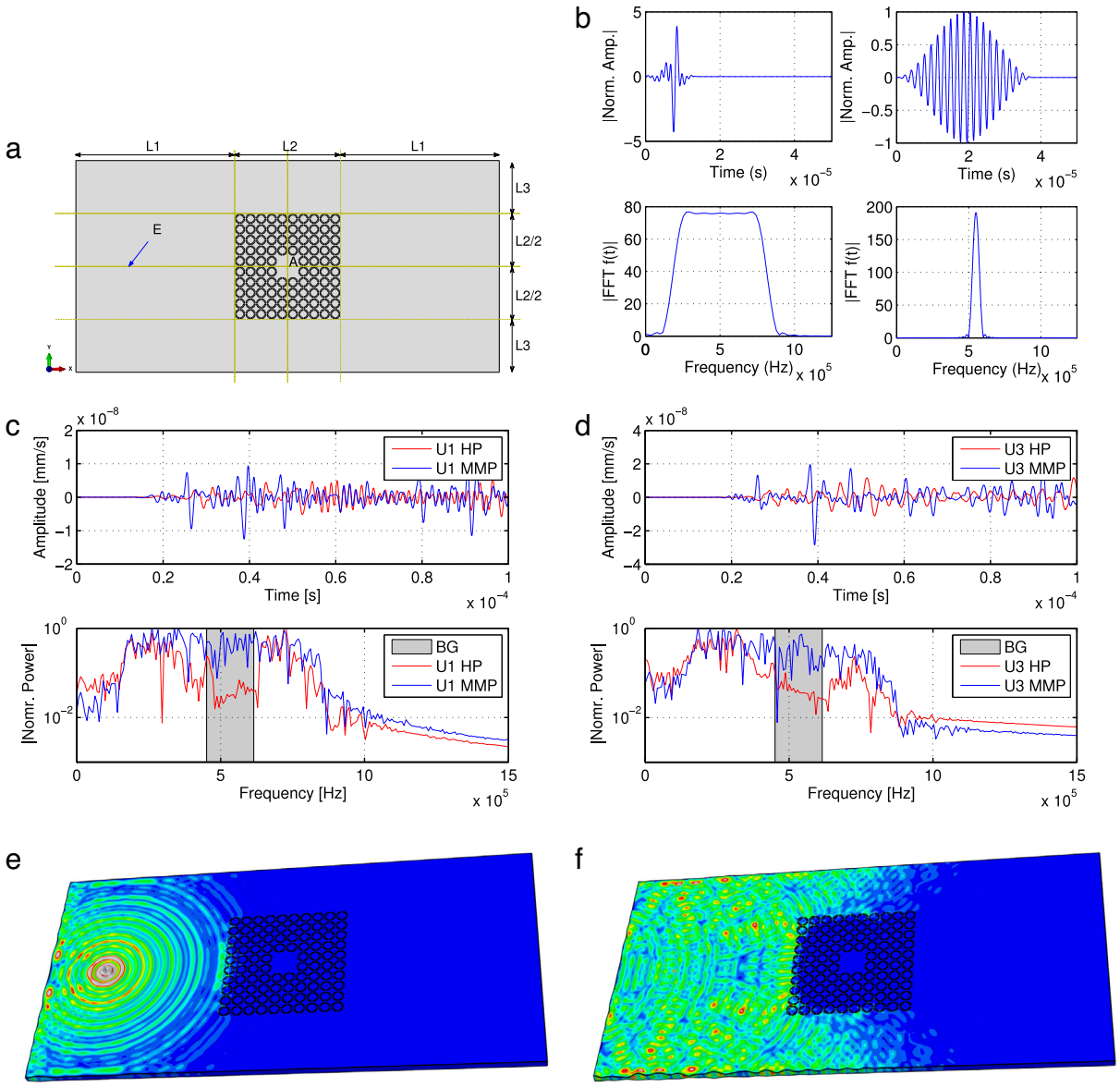

Fig. 7. (a) Schematic representation of a 3-D metamaterial plate (MMP) with a central region constituted by 4 rows of the proposed unit cells organized in a ring geometry around a homogeneous region. (b) Time and frequency content of the applied pulses. (c, d) Normalized displacements u_1 and u_3 at point A with corresponding Fourier spectrum in the MMP and in a reference homogeneous plate (HP). The BGs from the corresponding dispersion spectrum are highlighted by shaded regions. (e, f) Snapshots of the corresponding Von-Mises stress distribution in the MMP.

the designed metamaterial ring region are further highlighted by computing Von Mises stress maps for the excitation case (ii), i.e. a Hanning-modulated 21 sine cycle with central frequency 550 kHz shown in Fig. 7(e, f). Clearly, when the frequency content of stress waves falls inside the BG frequency range, the area inside the phononic region remains motionless, since all the waves are filtered out. Thus, we can conclude that the proposed metamaterial with quasi-resonant Bragg BGs is capable of attenuating elastic waves in a very efficient manner.

4. Conclusion

We have proposed and theoretically studied a novel BG formation mechanism in two- and single-phase phononic metamaterials. We show evidence that the resulting BGs can be twice as large as those of conventional Bragg BGs in the corresponding phononic structures with cavities. The BG widening effect is achieved by coupling a Bragg BG with local resonance effects in parts of the matrix material, rather than in inclusions as is commonly done. The resulting so-called 'quasi-resonant Bragg' BGs have been found in 2-D and 3-D slab-like metamaterial configurations. Parametric studies, in which geometric parameters and/or sample thickness have been varied, show that the dispersion relation is a typical one for known metamaterials with overlapping Bragg and local resonance BGs. Additional insight into BG formation mechanisms have been gained by analyzing vibrations patterns at the BG bounds and the imaginary part of the band structure diagrams. Moreover, transmission properties have been evaluated and demonstrate that the designed structures show enhanced wave attenuation abilities, making them suitable for noise abatement and vibration suppression applications. Further investigations are required in the future to gain deeper insight into the nature of this type of structure. However, considering the simplicity of the geometries involved, the elimination of the need for multiple phases and the proven reduced sensitivity to geometrical parameters of the inclusions, the proposed structures could already significantly simplify the man-

ufacture of real structures and thus be exploited in practical applications.

Acknowledgments

A.K. has received funding from the European Union's Seventh Framework programme for research and innovation under the Marie Skłodowska-Curie Grant Agreement No. 609402-2020 researchers: Train to Move (T2M). M.M. has received funding from the European Union's Horizon 2020 research and innovation programme under the Marie Skłodowska-Curie Grant Agreement No. 658483. N.M.P. is supported by the European Research Council as the PI of the following active projects: ERC StG Ideas 2011 BIHSNAM No. 279985; ERC PoC 2015 SILKENE No. 693670, and by the European Commission under the Graphene Flagship (WP14 "Polymer Nanocomposites", No. 604391). F.B. is supported by ERC StG Ideas 2011 BIHSNAM No. 279985. Computational resources were provided by HPC@POLITO (http://www.hpc.polito.it).

References

[1] S. Brûlé, E.H. Javelaud, S. Enoch, S. Guenneau, Experiments on seismic metamaterials: molding surface waves, Phys. Rev. Lett. 112 (2014) 133901.
[2] M. Miniaci, A. Krushynska, F. Bosia, N.M. Pugno, Large scale mechanical metamaterials as seismic shields, New J. Phys. 18 (2016) 083041.
[3] R. Mártinez-Sala, J. Sancho, J.V. Sánchez, J. Linres, F. Mesegure, Sound attenuation by sculpture, Nature 378 (1995) 241.
[4] M. Molerón, C. Daraio, Acoustic metamaterial for subwavelength edge detection, Nature Commun. 6 (2015) 8037.
[5] T. Gorishnyy, M. Maldovan, C. Ullal, E. Thomas, Sound ideas, Phys. World 18 (2005) 2–7.
[6] L. Brillouin, Wave Propagation in Periodic Structures, Dover, New York, 1946.
[7] N. Kaina, M. Fink, G. Lerosey, Composite media mixing Bragg and local resonances for highly attenuating and broad bandgaps, Sci. Rep. 3 (2013) 3240.
[8] R. Sainidou, N. Stefanou, A. Modinos, Formation of absolute frequency gaps in three-dimensional solid phononic crystals, Phys. Rev. B 66 (2002) 212301.
[9] M. Sigalas, M.S. Kushwaha, E.N. Economou, M. Kafesaki, I.E. Psarobas, W. Steurer, Classical vibrational modes in phononic lattices: theory and experiment, Z. Kristallogr. 220 (2005) 765–809.
[10] Z. Liu, X. Zhang, Y. Mao, Y. Zhu, Z. Yang, C. Chan, P. Sheng, Locally resonant sonic materials, Science 289 (2000) 1734–1736.
[11] Z. Liu, C.T. Chan, P. Sheng, Analytic model of phononic crystals with local resonances, Phys. Rev. B 71 (2005) 014103.
[12] M. Hirsekorn, Small-size sonic crystals with strong attenuation bands in the audible frequency range, Appl. Phys. Lett. 84 (2004) 3364–3366.
[13] P. Wang, F. Casadei, S. Shan, J.C. Weaver, K. Bertoldi, Harnessing buckling to design tunable locally resonant acoustic metamaterials, Phys. Rev. Lett. 133 (2014) 014301.
[14] A. Krushynska, V. Kouznetsova, M. Geers, Towards optimal design of locally resonant acoustic metamaterials, J. Mech. Phys. Solids 71 (2014) 179–196.
[15] J. Shim, S. Shan, A. Kosmrlj, S. Kang, E. Chen, J. Weaver, K. Bertoldi, Harnessing instabilities for design of soft reconfigurable auxetic/chiral materials, Soft Matter 9 (2013) 8198–8202.
[16] E. Baravelli, M. Ruzzene, Internally resonating lattices for bandgap generation and low-frequency vibration control, J. Sound Vib. 332 (2013) 6562–6579.
[17] L. Liu, M.I. Hussein, Wave motion in periodic flexural beams and characterization of the transition between Bragg scattering and local resonance, J. Appl. Mech. 79 (2011) 011003.
[18] L. Raghavan, A.S. Phani, Local resonance bandgaps in periodic media: Theory and experiment, J. Acoust. Soc. Am. 134 (2013) 1950–1959.
[19] B. Sharma, C. Sun, Local resonance and Bragg bandgaps in sandwich beams containing periodically inserted resonators, J. Sound Vib. 364 (2016) 133–146.
[20] Y. Xiao, J. Wen, D. Yu, X. Wen, Flexural wave propagation in beams with periodically attached vibration absorbers: Band-gap behavior and band formation mechanisms, J. Sound Vib. 332 (2013) 867–893.
[21] H. Zhao, Y. Liu, G. Wang, J. Wen, D. Yu, X. Han, X. Wen, Resonance modes and gap formation in a two-dimensional solid phononic crystal, Phys. Rev. B 72 (2005) 012301.
[22] C. Croënne, E.J.S. Lee, H. Hu, J.H. Page, Band gaps in phononic crystals: Generation mechanisms and interaction effects, AIP Adv. 1 (2011) 041401.
[23] T. Still, W. Cheng, M. Retsch, R. Sainidou, J. Wang, U. Jonas, N. Stefanou, G. Fytas, Simultaneous occurrence of structure-directed and particle-resonance-induced phononic gaps in colloidal films, Phys. Rev. Lett. 100 (2008) 194301.
[24] B. Yuan, V. Humphrey, J. Wen, X. Wen, On the coupling of resonance and Bragg scattering effects in three-dimensional locally resonant sonic materials, Ultrasonics 53 (2013) 1332–1343.
[25] J.H. Page, S. Yang, Z. Liu, M.L. Cowan, C.T. Chan, P. Sheng, Tunneling and dispersion in 3D phononic crystals, Z. Kristallogr. 220 (2005) 859–870.
[26] Y. Achaoui, A. Khelif, S. Benchabane, L. Robert, V. Laude, Experimental observation of locally-resonant and Bragg band gaps for surface guided waves in a phononic crystal of pillars, Phys. Rev. B 83 (2011) 104201.
[27] V. Leroy, A. Bretagne, M. Fink, H. Willaime, P. Tabeling, A. Tourin, Design and characterization of bubble phononic crystals, Appl. Phys. Lett. 95 (2009) 171904.
[28] Y. Chen, L. Wang, Periodic co-continuous acoustic metamaterials with overlapping locally resonant and bragg band gaps, Appl. Phys. Lett. 105 (2014) 191907.
[29] Y. Tanaka, Y. Tomoyasu, S. Tamura, Band structure of acoustic waves in phononic lattices: Two-dimensional composites with large acoustic mismatch, Phys. Rev. B 62 (2000) 7387–7392.
[30] B. Merheb, P.A. Deymier, M. Jain, M. Aloshyna-Lesuffleur, S. Mohanty, A. Berker, R.W. Greger, Elastic and viscoelastic effects in rubber/air acoustic band gap structures: A theoretical and experimental study, J. Appl. Phys. 104 (2008) 064913.
[31] S. Mohammadi, A.A. Eftekhar, A. Khelif, W.D. Hunt, A. Adibi, Evidence of large high frequency complete phononic band gaps in silicon phononic crystal plates, Appl. Phys. Lett. 92 (2008) 221905.
[32] Y. Liu, J.-Y. Su, Y.-L. Xu, X.-C. Zhang, The influence of pore shapes on the band structures in phononic crystals with periodic distributed void pores, Ultrasonics 49 (2009) 276–280.
[33] Y.-F. Wang, Y.-S. Wang, X.-X. Su, Large bandgaps of two-dimensional phononic crystals with cross-like holes, J. Appl. Phys. 110 (2011) 113520.
[34] M.K. Lee, P.S. Ma, I.K. Lee, H.W. Kim, Y.Y. Kim, Negative refraction experiments with guided shear-horizontal waves in thin phononic crystal plates, Appl. Phys. Lett. 98 (2011) 011909.
[35] Y.-F. Wang, Y.-S. Wang, Multiple wide complete bandgaps of two-dimensional phononic crystal slabs with cross-like holes, J. Sound Vib. 332 (2013) 2019–2037.
[36] D. Bigoni, S. Guenneau, A.B. Movchan, M. Brun, Elastic metamaterials with inertial locally resonant structures: Application to lensing and localization, Phys. Rev. B 87 (2013) 174303.
[37] R.P. Moiseyenko, Y. Pennec, R. Marchal, B. Bonello, B. Djafari-Rouhani, Broadband attenuation of lamb waves through a periodic array of thin rectangular junctions, Phys. Rev. B 90 (2014) 134307.
[38] R. Zhu, X.N. Liu, G.K. Hu, C.T. Sun, G.L. Huang, Negative refraction of elastic waves at the deep-subwavelength scale in a single-phase metamaterial, Nat. Commun. 5 (2014) 5510.
[39] X. Hu, C.T. Chan, J. Zi, Two-dimensional sonic crystals with Helmholtz resonators, Phys. Rev. E 71 (2005) 055601.
[40] Z.Y. Cui, T.N. Chen, J.H. Wu, H.L. Chen, B. Zhang, Measurements and calculations of two-dimensional band gap structure composed of narrowly slit tubes, Appl. Phys. Lett. 93 (2008) 144103.
[41] D.P. Elford, L. Chalmers, F.V. Kusmartsev, G.M. Swallowe, Matryoshka locally resonant sonic crystal, J. Acoust. Soc. Am. 130 (2011) 2746–2755.
[42] V. Romeo-García, J.V. Sánchez-Pérez, L.M. Garcia-Raffi, Tunable wideband bandstop acoustic filter based on two-dimensional multiphysical phenomena periodic systems, J. Appl. Phys. 110 (2011) 014904.
[43] J.S. Lee, S. Yoo, Y.K. Ahn, Y.Y. Kim, Broadband sound blocking in phononic crystals with rotationally symmetric inclusions, JASA Express Lett. 138 (2015) EL217–EL222.
[44] B. Yuan, V.F. Humphrey, J. Wen, X. Wen, On the coupling of resonance and Bragg scattering effects in three-dimensional locally resonant sonic materials, Ultrasonics 53 (2013) 1332–1343.
[45] A. Krushynska, V. Kouznetsova, M. Geers, Visco-elastic effects on wave dispersion in three-phase acoustic metamaterials, J. Mech. Phys. Solids 96 (2016) 29–47.